Hindawi Publishing Corporation
Mathematical Problems in Engineering
Volume 2016, Article ID 9475752, 7 pages
http://dx.doi.org/10.1155/2016/9475752

Research Article

Parameters in Multiphase Flowing of Natural Gas NGH Slurry via Vertical Pipe

Dai Maolin and Wu Kaisong

School of Mechatronic Engineering, Southwest Petroleum University, Chengdu, Sichuan 610500, China

Correspondence should be addressed to Wu Kaisong; wks9998@163.com

Received 9 April 2016; Accepted 15 June 2016

Academic Editor: Sandro Longo

In recent years, the pipeline flowing of natural gas hydrate (*hereinafter NGH*) slurry has been a promising technique of multiphase flowing via pipe and that of crushed hydrate mixture slurry is also a key technique in solid fluidization mining method of nondiagenetic NGH reservoir below the seabed. In this paper, by using similarity rules, a small-scale simulation model was established to shorten the calculation time. The correctness of the simulation model has been verified through comparison with experiment. Thereby, the distribution of velocity and volume fraction of each phase in the vertical pipe was obtained, and the prototype of vertical pipe was analyzed. By study on the pipe resistance, the pressure drop of slurry, when flowing in vertical pipe, could be calculated as $\Delta P = \rho g h + 0.23 C \rho v^{1.8}$. In the end, by adjusting volume fraction of particles in the mixture slurry, the relationship between the solid particles' volume fraction and piezometric pressure drop was obtained. When the optimal flow velocity of the slurry is 2 m/s and the ratio of NGH volume fraction to that of sand is 4 : 1, the optimal particle volume fraction ranges from 20% to 40%.

1. Introduction

As a new mineral resource, the huge carbon reserves of natural gas hydrate (*hereinafter NGH*) have been a well-concerning focus in the past decades. The occupancy volume of methane in NGH, estimated by experts overseas, is nearly 2.0×10^{16} m^3, twice the sum of carbon reserves in all oil, gas, coal, and other substances on earth [1–3]. Specifically, the reservoir of NGH in deep water is about 100 times of that in land [4]. And the hydrate in shallow layers of deep water is mostly the nondiagenetic one, accounting for 85% of the total amount below the seabed.

At present, the investigation of multiphase flow in pipeline mainly focuses on analyzing the pipe resistance in the process of fluid flow. The marine NGH investigated in this paper is the nondiagenetic one stored in shallow layers below the seabed. The NGH slurry crushed through solid fluidization [5] generally contains the sand, NGH, and seawater. However, the flow characteristics of such NGH slurry have not been studied yet. The only similar studies were those on the ice slurry, which merely concentrated on the flow characteristics of ice slurry in horizontal pipes [6, 7]. Jihong et al. [8] investigated the isothermal flow of ice slurry in vertical pipe and obtained the distribution of concentration and velocity of ice particles in the ice slurry. Lee et al. [9] experimentally studied the pipe resistance of ice slurry in different flow directions in vertical pipe and analyzed the impact of the particles concentration changes on the pipe resistance. By sampling the concentrations, Stamatiou and Kawaji [10, 11] detected the concentration distribution of the ice particles along a cross section of the pipe, but they did not provide a quantitative calculation method for the concentration distribution of the ice particles and the pipe resistance of the ice slurry.

Therefore, on the basis of an innovative solid fluidization mining technique of hydrate reservoir in shallow layers below the seabed, this paper investigated the flowing of crushed NGH mixture slurry, providing some valuable references for the experimental studies on the multiphase pipeline flowing of marine nondiagenetic NGH slurry.

2. Analysis of Pipeline Model

2.1. Similarity Rules. Since the calculation and analysis are complicated and enormous in the actual cases, in order to save time, a small-scale model is usually established by using similarity rules for the simulation testing. By observing the flow distributions of the model, the flow distributions and relevant data of the prototype can be inferred.

(1) Geometric Similarity. All linear dimensions of the model are related to the corresponding dimensions of the prototype by a constant scale factor. All angles are preserved [12]. Let the parameter subscripts of the model be with m and those of the prototype with n; then geometric similarity requires the following:

$$\delta_l = \frac{l_n}{l_m}. \tag{1}$$

And the area-scale ratio is as follows:

$$\delta_A = \frac{A_n}{A_m} = \frac{l_n^2}{l_m^2} = \delta_l^2. \tag{2}$$

(2) Kinematic Similarity. It means that, in the prototype and model, the corresponding kinematic parameters, such as the velocity and acceleration, are in the same direction and are proportional; then the time-scale ratio is as follows:

$$\delta_t = \frac{t_n}{t_m}. \tag{3}$$

The velocity-scale ratio is as follows:

$$\delta_v = \frac{v_n}{v_m} = \frac{\delta_l}{\delta_t}. \tag{4}$$

(3) Dynamic Similarity. It means that, in the prototype and model, the forces at corresponding points are in the same direction and are proportional; then the force-scale ratio is as follows:

$$\delta_F = \frac{F_n}{F_m} = \delta_\rho \delta_l^2 \delta_v^2, \tag{5}$$

and the density-scale ratio is as follows:

$$\delta_\rho = \frac{\rho_n}{\rho_m}. \tag{6}$$

In summary, the pressure-scale ratio is as follows:

$$\delta_P = \frac{P_n}{P_m} = \frac{F_n/A_n}{F_m/A_m} = \frac{(F_n/F_m)}{(A_n/A_m)} = \delta_\rho \delta_v^2. \tag{7}$$

2.2. Medium Physical Properties. The nondiagenetic NGH mixture slurry below the seabed consists of the sand, seawater, and NGH. Among them, the sand and NGH are solid particles, while seawater is liquid. The multiphase flow is considered as incompressible fluid without phase change in the pipeline. During the simulation process, the physical parameters of the used media are as follows: the density of seawater $\rho = 1025\,\text{kg/m}^3$, the dynamic viscosity of seawater $\mu = 1.72 \times 10^{-3}\,\text{kg/(m·s)}$, the density of sand $\rho = 2600\,\text{kg/m}^3$, the solids shear viscosity of sand $\mu = 2.35 \times 10^{-3}\,\text{kg/(m·s)}$, the density of NGH (including cavity) $\rho = 600\,\text{kg/m}^3$, and the solids shear viscosity of NGH $\mu = 1.47 \times 10^{-3}\,\text{kg/(m·s)}$; let the solid particles be spherical with a diameter of 5 mm.

2.3. Parameter Calculation of Pipeline. A simulation model of pipeline is established on the basis of similarity rules. Let the length-scale ratio be $\delta_l = 10$, let the time-scale ratio be $\delta_t = 1$, and let the density-scale ratio be $\delta_\rho = 1$.

There are

$$\begin{aligned} \delta_v &= \frac{v_n}{v_m} = \frac{\delta_l}{\delta_t} = 10, \\ \delta_P &= \frac{P_n}{P_m} = \delta_\rho \delta_v^2 = 100. \end{aligned} \tag{8}$$

Then

$$\begin{aligned} l_n &= 10 l_m, \\ v_n &= 10 v_m, \\ P_n &= 100 P_m. \end{aligned} \tag{9}$$

By substituting the given data into the above formulas, the diameter of the solid particles is 0.5 mm, the pipeline diameter d_m is 50 mm, and the length l_m is 1000 mm in the simulation model. The pipeline diameter is about $20''$ and the length is 30 meters in the prototype.

The pipeline adopted in the experimental simulation is vertical, and the fluid is incompressible. Given any pipe segment and sections at its inlet and outlet, the energy conservation equation could be expressed as follows:

$$E_{k_{\text{in}}} + E_{p_{\text{in}}} + E_{z_{\text{in}}} = E_{k_{\text{out}}} + E_{p_{\text{out}}} + E_{z_{\text{out}}} + E_f, \tag{10}$$

where E_k denotes the kinetic energy of the fluid at a section, E_p denotes the pressure energy of the fluid at a section, E_z denotes the potential energy of the fluid at a section, and E_f denotes the internal energy dissipation of the fluid through the pipe segment.

Let $\Delta E_k = E_{k_{\text{in}}} - E_{k_{\text{out}}}$, $\Delta E_p = E_{p_{\text{in}}} - E_{p_{\text{out}}}$, and $\Delta E_z = E_{z_{\text{out}}} - E_{z_{\text{in}}}$; then

$$\Delta E_k + \Delta E_p = \Delta E_z + E_f. \tag{11}$$

As suggested by (11), when the fluid is flowing in the pipe without phase change, its kinetic and pressure energy are converted into potential energy and internal energy dissipation in the pipe. Theoretically, according to the continuity equation, since the fluid velocity remains unchanged at the inlet and outlet of the pipe, its kinetic energy stays the same [13, 14] (i.e., $\Delta E_k = 0$). For any two segments of the same length in the same vertical pipe, the internal energy

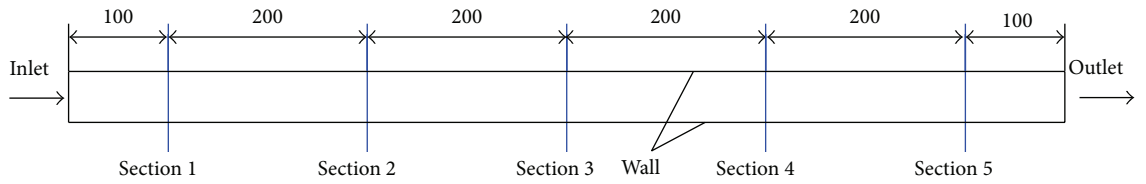

Figure 1: Pipe simulation model and its sections.

dissipation of the fluid and the potential energy difference in the two segments are equal; then the pressure drops in the two segments are equal.

Suppose the length of prototype pipe is H; then the pressure of fluid flow requires

$$P = \frac{H}{l_n} \cdot P_n = \frac{H}{l_m} \cdot \frac{\delta_\rho \delta_v^2}{\delta_l} \cdot P_m. \quad (12)$$

In other words, the pressure drop of fluid flow is

$$\Delta P = \frac{H}{l_n} \cdot P_n = \frac{H}{l_m} \cdot \frac{\delta_\rho \delta_v^2}{\delta_l} \cdot \Delta P_m. \quad (13)$$

3. Modeling and Simulation Analysis

3.1. Establishment of Simulation Model. The geometric objects of fluid domain are established, that is, a cylinder of 50 mm in diameter and 1000 mm in length. Then this fluid domain is divided into hexahedral meshes by the Sweep. The inlet is located at the bottom of the vertical pipe and the outlet at the top. The pipe simulation model and its sections are shown in Figure 1.

On the basis of pressure-based solver, a mixture multiphase flow model and a standard k-ε turbulence model [15] are selected. The standard wall function is applied near the wall of the pipeline. The media property and related physical parameters are defined. Its boundary conditions including the inlet boundary condition, outlet boundary condition, and wall boundary condition are that velocity-inlet is adopted at the inlet boundary, with an inlet initial velocity v_{in} of 1 m/s; pressure-outlet is adopted at the outlet boundary, with outlet gauge pressure of 0 MPa (operating pressure is set to 10 MPa); and no-slip wall is adopted, with roughness of 0.2 μm. The volume fraction of solid is set to 20%, and the ratio of NGH volume fraction to that of sand is 4 : 1. The diameter of all solid particles is 0.5 mm.

3.2. Verification of Simulation Model

3.2.1. Grid-Independence Verification. To verify the grid-independence of the simulation model, the model is divided into hexahedral meshes with four different numbers of grids. Then, in the premise of guarantee that the physical parameters and boundary conditions of the above media are the same, four numerical simulations are carried out to obtain the piezometric pressure drop between the inlet and outlet. Four different numbers of grids and corresponding pressure drops are listed in Table 1.

Table 1: Four different numbers of grids and corresponding pressure drops.

Situation	1	2	3	4
Numbers of grids	575,794	843,596	1,184,624	1,473,680
Piezometric pressure drop (Pa)	283.52	283.67	283.56	283.51

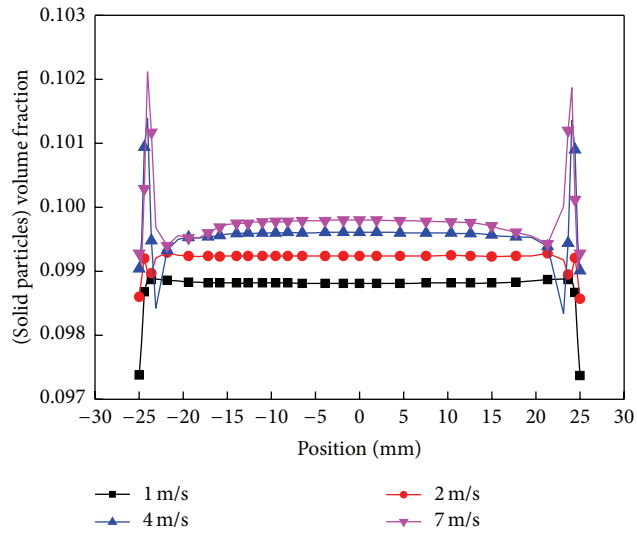

Figure 2: Distribution curves of the particles volume fraction along the diameter of the pipe.

As shown in Table 1, when the numbers of grids increase from 575,794 to 1,473,680, the piezometric pressure drops between the two ends are almost unchanged. It is to say that there is the grid-independence when the numbers of grids reach 575,794. For this reason, the numbers of grids in the simulation model are set to 575,794.

3.2.2. Verification of Simulation Model. Only the initial velocity of the inlet is changed in order to verify the simulation model of grid-independence. Section 3 is selected to get the distribution of the particles volume fraction in the slurry. The result is shown in Figure 2.

The results show that, during the flowing of slurry via vertical pipe, the particles volume fraction is symmetrically distributed along the diameter of the pipe. The particles volume fraction near wall is slightly lower than that in the core region. As the flow velocity of slurry increases, the particles

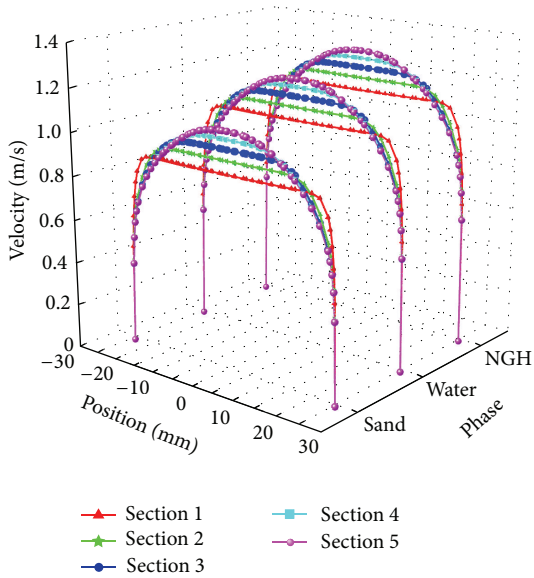

Figure 3: Distribution curves of velocity of each phase in the NGH slurry on different sections.

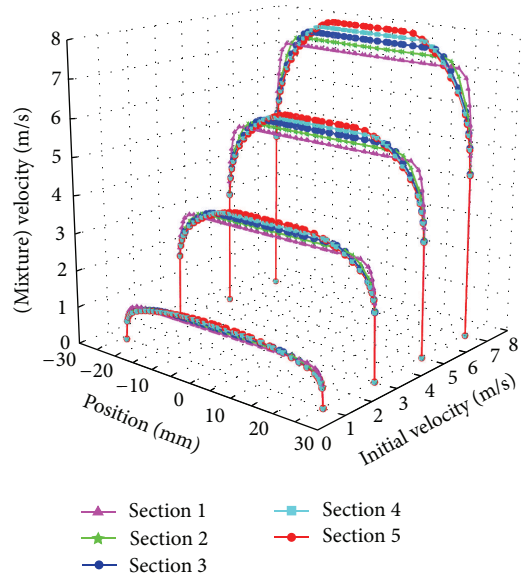

Figure 4: Distribution curves of the velocity of NGH slurry with initial velocities on different sections.

volume fraction in the core region gradually increases. The result is consistent with the distribution of the ice volume fraction of slurry in vertical pipe found by Jihong et al. [8], suggesting the feasibility and reliability of this simulation model in investigating the parameters in multiphase flow of marine NGH slurry via vertical pipe.

What is different is that the NGH slurry used in this study contains two types of solid particles with different densities, NGH and sand. When the flow velocity of NGH slurry is equal to or greater than 2 m/s, the particles volume fraction increases dramatically, followed by a sharp decline, and tended to be evenly distributed from the pipe wall to the axis of the pipe. Figure 2 also shows that the peak of particles volume fraction is near the wall.

3.3. Analysis of Numerical Results. Figure 3 shows the distribution curves of the velocity of each phase on different sections, when the flow velocity of NGH slurry is 1 m/s at the inlet. As shown in Figure 3, the velocity distribution of each phase in NGH slurry is symmetrical along the diameter of the sections and gradually increases from the wall to the axis of the pipe. When it is near the axis, the velocity tends to be constant. As the height of the sections increases, the curve of the velocity tends to be circular. This indicates that when the fluid is flowing via vertical pipe, the uneven distribution of its flow velocity becomes more significant along with the increase in height.

It can also be seen from Figure 3 that, on the same section, the velocity of the hydrate phase is greater than that of the sand phase. The velocity of the seawater phase is between the hydrate and sand. In other words, the flowability of hydrate particles in the slurry is higher than that of the seawater, but the sand particles are lower than the seawater.

At different initial velocities of NGH slurry, the distribution curves of the velocity of each section are shown in Figure 4. The distribution of the NGH slurry velocities is consistent with that of each phase on different sections by comparing Figure 3 with Figure 4. In the section of the same height, with the increase in the initial velocity, the distribution curves of velocity of NGH slurry tend to be more horizontal. The higher the section is from the inlet, the more obvious the tendency is. Figure 4 also implies that, with the increase of the initial velocity, the difference in velocities of adjacent two sections increases in the core region. Thus, increasing the initial velocity of the NGH slurry can exacerbate the uneven distribution of slurry velocities in vertical pipe.

Figures 5 and 6 show the distribution curves of the volume fractions of NGH and sand on different sections along the diameter. According to Figure 5, the distribution of NGH volume fraction is even in the core region of pipe. The NGH volume fraction gradually increases along with the initial velocity increasing. Similarly, as shown in Figure 6, the distribution of sand volume fraction is even in the core region of pipe. But its volume fraction declined with the initial velocity increasing. This is because, as the initial velocity increases, the sand particles gradually move closer to the wall, resulting in NGH volume fraction increases and sand volume fraction decreases in the core region of pipe. When the initial velocity is 1 m/s, the distribution of NGH volume fraction has the shape of "$\prod$." When the initial velocity is equal to or greater than 2 m/s, the distribution of NGH volume fraction has the shape of "$\coprod$."

According to Figures 5 and 6, as the initial velocity increases, the volume fractions of NGH and sand particles fluctuate more significantly near the wall, further verifying that increasing the initial velocity of the NGH slurry can exacerbate the uneven distribution of slurry velocities in vertical pipe. However, at the same initial velocity, the distribution curves of volume fraction of NGH or sand on

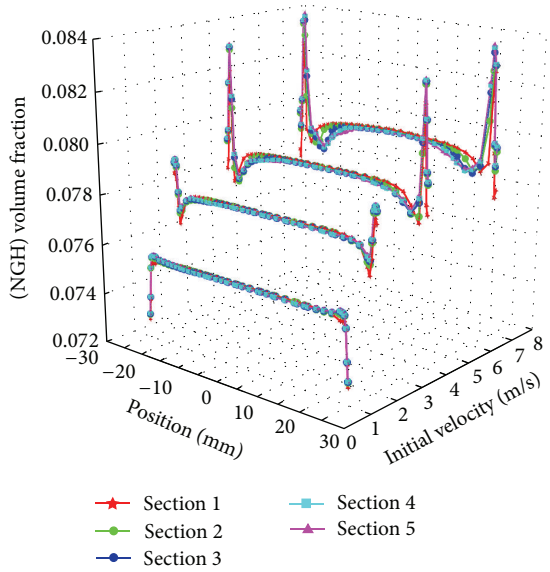

FIGURE 5: Distribution curves of the NGH volume fraction along the diameter on different sections.

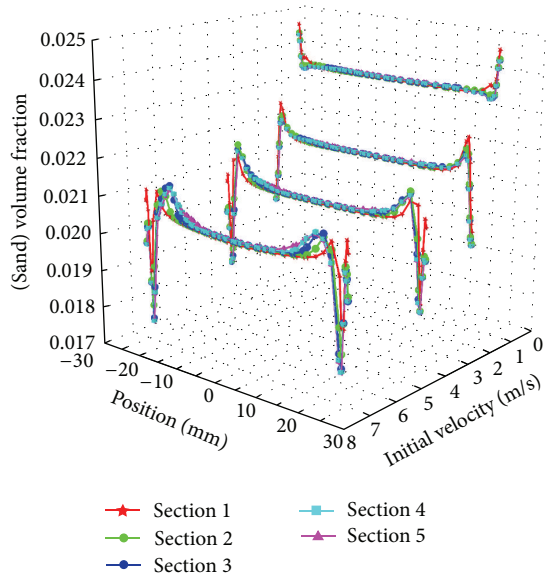

FIGURE 6: Distribution curves of the sand volume fraction along the diameter on different sections.

different sections tend to be consistent. Suggesting that the height of slurry in vertical pipe barely affected the distribution of the volume fraction of NGH or sand.

3.4. Calculation of Prototype. According to the numerical result analysis in Section 3.3, when the initial velocity is 2 m/s, the distribution curve of flow velocity of NGH slurry and the volume fraction of NGH and sand are even in vertical pipe. In the simulation model, the optimal initial velocity of NGH slurry is $v_m = 2$ m/s, and the corresponding piezometric pressure drop is $\Delta P_s = 809.35$ Pa.

Then, in the prototype, the actual flow velocity is

$$v_n = 10v_m = 20 \text{ m/s}. \tag{14}$$

For nongaseous medium, when the gravity is taken into consideration, the piezometric head is the sum of the pressure head and elevation head of the fluid; that is,

$$P_s = P + P_z, \tag{15}$$

where P_s denotes the piezometric pressure of the fluid at a section.

Let $\Delta P_s = P_{s_{\text{in}}} - P_{s_{\text{out}}}$, $\Delta P = P_{\text{in}} - P_{\text{out}}$, and $\Delta P_z = P_{z_{\text{out}}} - P_{z_{\text{in}}}$; then

$$\Delta P = \Delta P_s + \Delta P_z. \tag{16}$$

And the elevation pressure difference in the pipeline is

$$\Delta P_z = \rho g h = 9996 \text{ Pa}. \tag{17}$$

So the pressure drop in the pipeline of simulation model is

$$\Delta P = \Delta P_s + \Delta P_z = 10805.35 \text{ Pa}. \tag{18}$$

Meanwhile the actual pressure drop in the pipeline is

$$\Delta P = \frac{H}{l_m} \cdot \frac{\delta_\rho \delta_v^2}{\delta_l} \cdot \Delta P_m = 3.24 \text{ MPa}. \tag{19}$$

4. Analysis of Flow Resistance

Figure 7 shows the relationship between the initial velocities and the piezometric pressure drop in the pipeline. As the initial velocity increases, the piezometric pressure drop also increases, and the rate of increase of piezometric pressure drop is elevating. The low initial velocity slows down the increase of piezometric pressure drop. This is because when the fluid flows slowly in the pipeline, the fluctuation of particles volume fractions decreases near the wall, and the distribution of particles volume fractions is even on the sections, and the NGH particles are subjected to buoyancy. At this moment, the internal energy dissipation of the fluid decreases through the pipe segment. With the initial velocity increasing, the particles volume fractions fluctuate more dramatically near the wall, leading to increased dissipation of internal energy and accelerated rate of increase of piezometric pressure drop.

By fitting the curve in Figure 7, the curve fitting data are obtained as listed in Table 2. The relationship between the slurry flow velocity and the piezometric pressure drop can be expressed as follows:

$$y = 0.23\rho x^{1.8}. \tag{20}$$

The major factors affecting the piezometric pressure drop in the pipeline also include pipe friction, pipe length, and medium parameters. In (20), in order to guarantee the dimension consistency on both sides of the equation, the

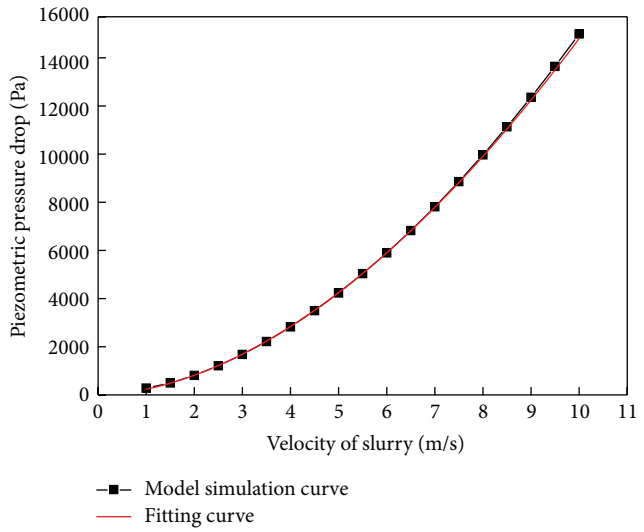

Figure 7: Relation curve of initial velocity to piezometric pressure drop.

Table 2: Curve fitting data.

Model	Allometric 1	Value	Standard error
Equation	$y = a\rho x^b$		
Adj. R-Square	0.9998		
	a	0.23	0.00325
	b	1.8	0.00659
	ρ	1020	0

coefficient C is introduced, in unit of $m^{-0.8}s^{-0.2}$. The coefficient C is related to pipe friction and medium parameters. When the particles volume fraction in the slurry is 0.2, coefficient C is 1. Then

$$\Delta P_s = 0.23C\rho v^{1.8}. \quad (21)$$

Since $\Delta P_z = \rho gh$, the pressure drop in the pipe is expressed as follows:

$$\Delta P = \rho gh + 0.23C\rho v^{1.8}. \quad (22)$$

5. Analysis of Pipeline Flow Parameters

Through analyzing the prototype in Section 3.4, the NGH slurry initial velocity in the simulation model is 2 m/s. In the premise of retaining the ratio of NGH volume fraction to that of sand being 4 : 1, the particles volume fraction is changed. The above simulation model is used for calculation, and the relationship between the particles volume fraction and the piezometric pressure drop is shown in Figure 8.

According to Figure 8, as the particles volume fraction increases, the piezometric pressure drop decreases firstly and then increases. This is because when the particles volume fraction is low, the distribution of particles volume fraction is even on the sections, and the NGH accounts for the majority of the solid particles, whose density are lower than that of seawater. In the flow process, the NGH particles are subjected

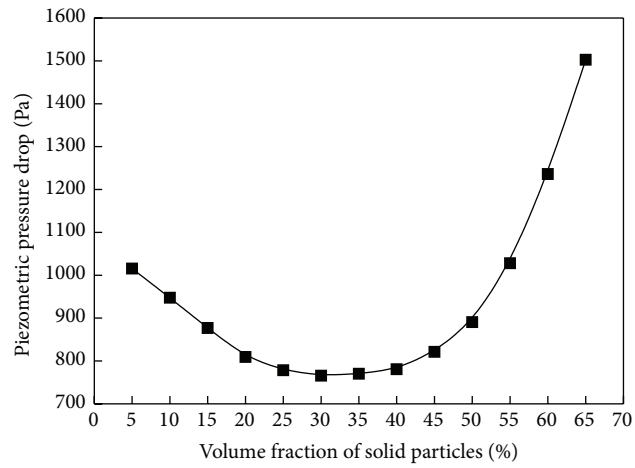

Figure 8: Relation curve of the particles volume fraction to the piezometric pressure drop.

to buoyancy, reducing the piezometric pressure drop in the pipe. As the particles volume fraction continues to increase, the distribution of particles volume fraction on the sections becomes more uneven, which plays a dominant role in the flow process and increases shear stress among the fluid, and increases the piezometric pressure drop dramatically.

It can also be seen from Figure 8 that when the particles volume fraction ranges in 20%~40%, the curve of the piezometric pressure drop tends to be flat. Therefore, in the prototype, the particles volume fraction should be controlled at 20%~40% to ensure the stable flow in vertical pipe, as well as to achieve a minimum flow pressure.

6. Conclusions

(1) The higher the slurry flows in vertical pipe is, the more uneven the flow velocity becomes for each phase along diameter of section.

(2) When natural gas hydrate (NGH) slurry flows in vertical pipe, the flowability of NGH particles is higher than that of the sand particles, and the flowability of seawater falls between those of NGH and sand particles.

(3) As the NGH slurry initial velocity increases, the particles volume fraction fluctuates more significantly near the wall, leading to a rapid increase in the piezometric pressure drop.

(4) By fitting the curve, the relationship between the piezometric pressure drop and the initial velocity is obtained as $\Delta P_s = 0.23C\rho v^{1.8}$, and then the expression of the pressure drop is obtained as $\Delta P = \rho gh + 0.23C\rho v^{1.8}$.

(5) The similarity rules are employed to calculate pipeline flow parameters in the prototype. In the 20″ pipe, the optimal initial velocity of the slurry is 20 m/s, the actual pressure drop in the pipeline of 30 m is 3.24 MPa, and the particles volume fraction is

controlled at 20%~40% to ensure the stable flow in vertical pipe.

Competing Interests

The authors declare that they have no competing interests.

Acknowledgments

The authors wish to express their appreciation to the School of Mechatronic Engineering, Southwest Petroleum University. This work was also supported by the National Natural Science Foundation of China (L1322021) and the Joint Funds of the Chinese Academy of Engineering (2013-04-ZCQ-002).

References

[1] K. A. Kvenvolden and T. D. Lorenson, "The global occurrence of natural gas hydrate," in *Natural Gas Hydrates: Occurrence, Distribution, and Detection*, C. K. Paull and W. P. Dillon, Eds., vol. 124 of *American Geophysical Union Geophysical Monograph*, pp. 3–18, American Geophysical Union, Washington, DC, USA, 2001.

[2] Y. G. Ye and C. L. Liu, *Natural Gas Hydrate: Experimental Techniques and Their Applications*, Springer, New York, NY, USA, 2013.

[3] K. A. Kvenvolden and T. D. Lorenson, "The global occurrence of natural gas hydrate," in *Natural Gas Hydrates: Occurrence, Distribution, and Detection*, American Geophysical Union, Washington, DC, USA, 2001.

[4] Z. Shouwei and L. Qingping, *Marine Engineering Design Guidelines: Deep Water Natural Gas Hydrates*, Petroleum Industry Press, Beijing, China, 2010.

[5] Z. Shouwei, C. Wei, and L. Qingping, "The green solid fluidization development principle of natural gas hydrate stored in shallow layers of deep water," *China Offshore Oil and Gas*, vol. 26, no. 5, pp. 1–7, 2014.

[6] A. Kitanovski, D. Vuarnoz, D. Ata-Caesar, P. W. Egolf, T. M. Hansen, and C. Doetsch, "The fluid dynamics of ice slurry," *International Journal of Refrigeration*, vol. 28, no. 1, pp. 37–50, 2005.

[7] A. C. S. Monteiro and P. K. Bansal, "Pressure drop characteristics and rheological modeling of ice slurry flow in pipes," *International Journal of Refrigeration*, vol. 33, no. 8, pp. 1523–1532, 2010.

[8] W. Jihong, Z. Tengfei, W. Shugang et al., "Numerical simulation of ice slurry flow in a vertical pipe," *Journal of Refrigeration*, vol. 33, no. 2, pp. 42–46, 2012.

[9] D. W. Lee, C. I. Yoon, E. S. Yoon et al., "Experimental study of flow and pressure drop of ice slurry for various pipes," in *Proceedings of the 5th Workshop on Ice-Slurries of the International Institute of Refrigeration*, Stockholm, Sweden, 2002.

[10] E. Stamatiou and M. Kawaji, "Thermal and flow behavior of ice slurries in a vertical rectangular channel. Part I: local distribution measurements in adiabatic flow," *International Journal of Heat and Mass Transfer*, vol. 48, no. 17, pp. 3527–3543, 2005.

[11] E. Stamatiou and M. Kawaji, "Thermal and flow behavior of ice slurries in a vertical rectangular channel. Part II. Forced convective melting heat transfer," *International Journal of Heat and Mass Transfer*, vol. 48, no. 17, pp. 3544–3559, 2005.

[12] F. M. White, *Fluid Mechanics*, McGraw-Hill, New York, NY, USA, 7th edition, 2009.

[13] Y. Enxi, *Engineering Fluid Mechanics*, Petroleum Industry Press, Beijing, China, 2009.

[14] Z. Yexun, H. Baoqing, Y. Gongbai et al., "Scientific value and application of similar elements in geomatics," *Journal of Guilin University of Technology*, vol. 34, no. 4, pp. 732–736, 2014.

[15] K. A. Hafez, O. A. Elsamni, and K. Y. Zakaria, "Numerical investigation of the fully developed turbulent flow over a moving wavy wall using κ-ε turbulence model," *Alexandria Engineering Journal*, vol. 50, no. 2, pp. 145–162, 2011.